



Published in final edited form as:

Mol Cancer Ther. 2020 January ; 19(1): 147–156. doi:10.1158/1535-7163.MCT-18-1202.

Dual inhibition of angiopoietin-TIE2 and MET alters the tumor microenvironment and prolongs survival in a metastatic model of renal cell carcinoma

May Elbanna^{1,#}, Ashley R. Orillion^{1,2,#}, Nur P. Damayanti¹, Remi Adelaiye-Ogala^{1,3}, Li Shen⁴, Kristen Marie Miles⁵, Sreenivasulu Chintala¹, Eric Ciamporcerro⁶, Swathi Ramikrishnan³, Sheng-yu Ku³, Karen Rex⁷, Sean Caenepeel⁷, Angela Coxon⁷, Roberto Pili^{1,*}

¹Genitourinary Cancers Program, Melvin and Bren Simon Cancer Center, Indiana University, Indianapolis, IN USA

²Department of Cellular and Molecular Biology, University at Buffalo, Roswell Park Cancer Institute, Buffalo, NY USA

³Department of Cancer Pathology and Prevention, University at Buffalo, Roswell Park Cancer Institute, Buffalo, NY USA

⁴Department of Medicine, Roswell Park Cancer Institute, Buffalo, NY USA

⁵Center for Personalized Medicine, Roswell Park Cancer Institute, Buffalo, NY USA

⁶Department of Medicine and Experimental Oncology, University of Turin, Turin Italy

⁷Oncology Research, Amgen Inc, Thousand Oaks, CA USA.

Abstract

Receptor tyrosine kinase inhibitors have shown clinical benefit in clear cell renal cell carcinoma (ccRCC) but novel therapeutic strategies are needed. The angiopoietin/Tie2 and MET pathways have been implicated in tumor angiogenesis, metastases, and macrophage infiltration. In our study, we used trebananib, an angiopoietin 1/2 inhibitor and a novel small molecule MET kinase inhibitor in patient derived xenograft (PDX) models of ccRCC. Our goal was to assess the ability of these compounds to alter the status of tumor infiltrating macrophages, inhibit tumor growth and metastases, and prolong survival. Seven-week-old SCID mice were implanted subcutaneously or orthotopically with human ccRCC models. One month post implantation, mice were treated with angiopoietin 1/2 inhibitor trebananib (AMG 386), MET kinase inhibitor or combination. In our metastatic ccRCC PDX model, RP-R-02LM, trebananib alone and in combination with a MET kinase inhibitor significantly reduced lung metastases and M2 macrophage infiltration (p=0.0075 and p=0.0205 respectively). Survival studies revealed that treatment of the orthotopically implanted RP-R-02LM tumors yielded a significant increase in survival in both trebananib and combination groups. Additionally, resection of the subcutaneously implanted primary tumor

* **Corresponding Author:** Roberto Pili, MD, Indiana Genitourinary Cancers Research Consortium, Melvin and Bren Simon Cancer Center, Indiana University, 535 Barnhill Drive, Room 455D, Indianapolis, IN, 317-278-7776, rpili@iu.edu.

#These authors equally contributed to the work

allowed for a significant survival advantage to the combination group compared to vehicle and both single agent groups. Our results show that the combination of trebananib with a MET kinase inhibitor significantly inhibits the spread of metastases, reduces infiltrating M2 type macrophages, and prolongs survival in our highly metastatic ccRCC PDX model, suggesting a potential use for this combination therapy in treating patients with ccRCC.

Keywords

c-Met; Angiopoietin; ccRCC; patient-derived xenograft; metastatic ccRCC; metastases

INTRODUCTION

Kidney cancer remains among the top ten most diagnosed cancers in both men and women, with >62,000 new cases of kidney cancer and >14,000 deaths anticipated in 2019. Of those cases, approximately 15% will develop aggressive metastatic disease (1,2). Clear cell renal cell carcinoma (ccRCC) is the most commonly diagnosed (70%) form of kidney cancer (1,2). Among those patients diagnosed with sporadic ccRCC, the majority has loss of function mutations in the *VHL* (von Hippel-Landau) tumor suppressor gene (3) resulting in an inability to functionally degrade the transcription factors HIFs (hypoxia inducible factors). This loss leads to overexpression of HIF-target genes, including vascular endothelial growth factor (VEGF), platelet-derived growth factor, hepatocyte growth factor (HGF), and the receptor tyrosine kinase mesenchymal-epithelial transition factor (MET), which drive tumor progression, metastases, and hyper-vascularization (4).

Tumor associated macrophages (TAMs) play a supporting role for kidney cancer. TAMs directly stimulate tumor growth, promote angiogenesis, support escape of immune surveillance, and assist in tumor cell dissemination (4–8). Further, increased presence of TAMs in the tumor microenvironment (TME) is correlated with poor prognosis in ccRCC patients (5). Production of immunosuppressive cytokines and extra cellular matrix remodeling enzymes, i.e. fibronectin, tenascin-c and matrix metalloproteinases by TAMs allow the tumor immune escape and assist in the epithelial to mesenchymal transition and dissemination of metastatic cells (4–6). TAMs are attracted to the TME by CCR2 signaling and subsequently differentiate into perivascular macrophages by help of CXCL12 and CXCR4 which are released by tumor cells and perivascular fibroblasts respectively (9). Anchorage of Tie2 expressing macrophages to the perivascular space is driven by Tie2-angiopoietin signaling (7,10–12).

Metastatic disease remains the leading cause of ccRCC related deaths with the most common sites being the lungs, bones and lymph nodes (2,13). Vascular stabilization and enhanced pericyte recruitment, while often reported to enhance tumor growth, have been recently linked to inhibition of tumor metastases, suggesting a dual potential role for the inhibition and stabilization of vasculature by pericytes (8,14–17).

The angiopoietin/Tie2 axis plays a significant role in the anchorage of TAMs to the perivascular space which significantly contributes to the maturation/disruption of tumor vasculature (18–20). Angiopoietin 1 (Ang1) activates the tyrosine kinase receptor, TIE2, and

affects the response of endothelial cells to VEGF (13, 19). Ang1/Tie2 interaction leads to blood vessel maturation and stabilization in both normal and tumor tissues (21,22). In the TME, Ang1 has been shown in few studies to both promote tumor growth and inhibit metastasis (23,24). Conversely, Tie2 receptor expressed by perivascular TAMs plays a key role in regulating Ang2 mediated vascular destabilization and sprouting in tumors (12).

Preclinical studies in colorectal cancer, breast cancer, and melanoma models have shown that inhibition of Ang2 resulted in reduced blood vessels, increased pericyte coverage, blood vessel stabilization, and altered EMT pathway activation (12,14,15,22). On the other hand, studies on Ang1 inhibition draw conflicting results on whether it induces or suppresses postnatal angiogenesis which suggests a context dependent function of Ang1 that require further investigation in order to be therapeutically harnessed (25). Therefore, although the regulation of angiogenesis through the Ang-Tie2 pathway has been well characterized, there is a lack of understanding of the crucial role that this pathway plays in metastatic disease.

The MET/HGF (c-MET) pathway is upregulated in 60–70% of ccRCC tumors leading to increased cell proliferation and metastatic potential (26). Recent reviews of MET addicted tumors indicate that MET/HGF inhibitors impact both the stroma and cancer cells. While MET/HGF inhibitors can directly inhibit tumor growth; these targeted agents may attenuate the efficacy of stromal cells, such as tumor-associated neutrophils and cytotoxic T cells, which inhibit tumor growth through upstream MET signaling (27,28). HGF also plays a key role downstream of the Ang/Tie2 axis by inducing pericyte recruitment, and vascular maturation (19). The MET pathway is also implicated in epithelial to mesenchymal transition (EMT), which is involved in tumor metastases (26,29). MET has also been reported to play a crucial role in the disruption of E-cadherin-based cell-cell contacts, thus affecting the TME in addition to the tumor niche (3,27).

The concept of combining inhibitors of both the MET and Ang/Tie2 pathways as treatment for metastatic ccRCC is postulated to be efficacious on both the tumor niche and the TME (1,17,30–32). The purpose of the current study was to examine the efficacy of this novel combination in pre-clinical ccRCC models. Overall, our data suggest that combination of dual Ang1/2 inhibitor (trebananib)(25) and a MET kinase inhibitor (compound 22) (33) increases trebananib induced anti-metastatic activity in a metastatic ccRCC model.

MATERIALS AND METHODS

Cell lines

The murine renal cell carcinoma cell line RENCA was initially purchased from American Type Culture Collection (National Cancer Institute) and stably tagged with a luciferase reporter in Dr. Pili's laboratory. Cells were cultured in RPMI 1640 (Corning) with 10% fetal bovine serum (Corning) and 1% Pen/Strep (LifeTechnologies) and incubated in 37C in an incubator containing 5% CO₂. Non-confluent cells were harvested using 0.25% Trypsin (Corning) and suspended in matrigel (Corning) and DPBS (Gibco) in a 1:1 ratio, 10ul containing 1×10⁴ cells was injected under the renal capsule. Mice were serially imaged using a bioluminescent IVIS imaging machine.

Mouse studies

All procedures were approved and performed in strict accordance with the Institutional Animal Care and use Committee (IACUC) at Roswell Park Cancer Institute and with the NIH Guide for the Care and Use of Laboratory Animals guidelines.

In vivo tumor growth (RENCA).—Five- to six- week old Balb/c mice (National Cancer Institute) were kept in a temperature controlled room on a 12/12-hour light /dark schedule with food and water *ad libitum*. Non-confluent RENCA-Luc cells were harvested using 0.25% Trypsin (Corning) and suspended in matrigel (Corning) and DPBS (Gibco) in a 1:1 ratio, 10 μ l containing 1×10^4 cells was injected under the renal capsule. Animals were randomly distributed into four groups: vehicle (soy bean oil), trebananib (Amgen386), a MET kinase inhibitor (compound 22), or combination. Mouse tumors were serially imaged using a bioluminescent IVIS imaging machine. Trebananib and compound 22 were provided by Amgen.

Xenograft models: Wild type male ICR Severe Combined Immune-deficient (SCID) mice, ages 6–8 weeks, were purchased from Charles River and housed in a sterile, pathogen-free facility and maintained in a temperature controlled room under a 12-hour light/dark schedule with food and water *ad libitum*. Upon arrival and acclimation mice were implanted orthotopically or subcutaneously ($\sim 1\text{mm}^2$ tumor piece) with RP-R-01, RP-R-02, or RP-R02LM which, were established from the skin metastasis of a patient with sporadic ccRCC which developed sunitinib resistance and skin metastasis from a patient with hereditary VHL syndrome ccRCC, respectively (34) (35).

Trebananib and MET kinase inhibitor treatment

Mice in the vehicle group were given soy bean oil daily (5d/week) by oral gavage. Mice in the treatment groups were treated with 5.6 mg/kg of trebananib (AMG 386) (25), twice a week i.p., and/or 30 mg/kg of MET kinase inhibitor (compound 22) (33), 5 days a week by oral gavage. In the sunitinib resistant studies, RP-R-01 and RP-R-02, mice were treated with 40 mg/kg of sunitinib for three weeks, or until tumor progression. Following this, the mice were treated with trebananib, MET kinase inhibitor, or a combination of both.

Histologic and immunohistochemical analysis

Tumor tissue specimen from each treatment group were fixed for 24 hours in formalin, paraffin-embedded and sectioned (5 μ m). Slide sections were deparaffinized and rehydrated via gradient alcohol washes. Antigen unmasking was performed by boiling slides in sodium citrate buffer (pH=6.0). Slides were subsequently incubated in hydrogen peroxide to reduce endogenous activity. For probing of the tissue for the proteins of interest, tissue sections were blocked in 2.5% horse serum (Vector Laboratories), and incubated overnight in primary antibodies against CD31 (1:100, Dianova). Following primary antibody incubation, slides were incubated with horseradish-peroxidase (HRP)-conjugated anti-rat antibody according to the manufacturer's protocol (Vector Laboratories). Following this slides were subjected to enzymatic development in diaminobenzidine (DAB). Sections were then dehydrated and mounted with cyto seal 60 (Thermo Scientific). Stained sections were imaged under bright field (IHC) using the Zeiss Axio microscope. The positive fields were

calculated in a blinded fashion by analyzing four random 20x fields per tissue and quantified using ImageJ software (36).

Lung tissues were paraffin embedded, sectioned and stained with hematoxylin and eosin stain to quantify the presence of micro-metastases. Lungs tissues were sectioned from the front, middle, and back of the lungs in order to obtain an overall assessment of the presence of lung metastases. Measurements were then performed in a blinded manner using ImageJ, where the total number and the diameter of micro-metastases were measured in 5–6 areas of each sectioned lung. Five images of each section of the lungs were taken (~30 images / lung). There were six lungs for each group (~720 images used in analysis).

Western blot analysis

Tumors from each treatment group were lysed in RIPA buffer (Sigma-Aldrich) containing protease and phosphatase inhibitor cocktails (Pierce). Protein concentrations were assessed using a standard BSA assay (Bio-Rad). 50 µg of protein from each sample was subjected to electrophoresis on 10% SDS-polyacrylamide gels (Bio-Rad) and transferred onto nitrocellulose membranes. Proteins of interest were detected with the following primary antibodies: E-cadherin (1:1000; Cell Signaling Technology), NG2 - Chondroitin Sulfate Proteoglycan (1:1000; EMD Millipore), phosphor-p44/42 MAPK (Erk1/2) (Thr202/Tyr204) (1:1000; Cell Signaling Technology), phosphor-AKT (Ser473) (1:1000; Cell Signaling Technology), GAPDH (1:1000; Cell Signaling Technology). Following incubation with primary antibody the membranes were probed with HRP-conjugated secondary antibodies (Bio-Rad) and exposed to chemiluminescence according to the manufacturer's instructions (Thermo Fisher Scientific) and exposed to film.

Quantitative real-time PCR

Total RNA was isolated from tumor samples according to manufacturer's instructions using TRIzol (Life Technologies) and measured using nano-drop technology. Quantitative RT-PCR was performed with E-cadherin and Snail primers (IDT-Technologies). Samples were denatured at 95°C for 10 seconds, annealed at 60°C for 30 seconds, and extended at 72°C for 1 minute using the Applied Biosystems 7900HT fast real time PCR system (Applied Biosystems). Sequence Detection Systems software v2.3 was used to identify the cycle threshold (C_t) values and to generate gene expression curves. Data were normalized to GAPDH expression and fold change was calculated.

Immunofluorescence staining

Tissue sections were prepared as described previously and stained for anti-rat CD31 (Dianova) at a 1:50 dilution and anti-rabbit NG2 at a 1:50 dilution overnight at 4°C. Following the primary incubation, slides were incubated with conjugated secondary antibodies – anti-rabbit FITC and anti-rat Cy5, co-stained with DAPI and mounted using Vectashield immunofluorescence mounting reagent. At least 5 images/tumor (referred to as fields of view) were acquired for at least 5 tumor pieces per group. High power fields were randomly and blindly taken to reflect the entire tumor. Analysis of the NG2 CD31 co-staining was performed in a blinded manner utilizing ImageJ software.

Confocal microscopy

CD31 and NG2 co-staining was performed on thicker sections of tumor tissue (μm) as described above. The Indiana Center for Biological Microscopy at IUPUI assisted in acquiring confocal images of the co-stained sections.

Statistical analysis

All statistical analyses were performed using GraphPad Prism7 software for Windows. Analysis of survival was conducted using the Kaplan-Meier method. Differences in treatment group survivals were assessed with the log-rank test. All other statistical analyses in this study were performed between experimental groups using the Student's T test with Welch's correction.

A p-value <0.05 was considered statistically significant.

RESULTS

Combined inhibition of Ang1/Ang2 and MET significantly reduces spontaneous lung metastases in the patient derived xenograft model RP-R-02LM.

To assess the efficacy of combining Ang1/Ang2 inhibition and MET kinase inhibition on primary tumor growth, we utilized two patient derived xenograft (PDX) models, RP-R-01 and RP-R-02 (29) in addition to the luciferase tagged syngeneic orthotopic murine model of renal cell carcinoma RENCA-Luc (37) As a MET inhibitor we utilized compound 22 which was previously reported to have selective kinase inhibitory activity (Supplementary Figure 1A,B) (33). The PDX models have been detailed previously as maintaining their original clear cell morphology, *VHL*-negative status, human *Alu* positive status, and containing common ccRCC gene mutations (34). Clinically effective first line therapeutics such as VEGF-targeting sunitinib elicit anti-tumor responses in ccRCC patients. However, the majority of patients who initially respond to sunitinib develop resistance and their tumors progress on treatment (34,38). Thus, we examined the treatment of sunitinib sensitive and sunitinib resistant models with trebananib and cMET inhibition to assess the efficacy of this novel combination. Our preliminary experiments assessed the primary tumor growth of RP-R-01, RP-R-02LM (intrinsically sunitinib resistant) and RENCA-Luc tumors. When the tumors reached a detectable size, 100–150mm³ for the subcutaneous PDX models approximately or 1–3 $\times 10^5$ average radiance for RENCA mice were randomized into four groups: vehicle (soy bean oil), trebananib, MET kinase inhibitor (compound 22), and combination. Mice were treated with 5.6 mg/kg subcutaneous injections of trebananib twice a week and/or 30 mg/kg MET kinase inhibitor by oral gavage 5 days a week. In the RP-R-02LM model (35), which spontaneously metastasizes to the lungs when implanted subcutaneously or orthotopically, we found that although MET kinase inhibitor treated tumors trended towards a decrease in end of treatment size in comparison to vehicle and combination groups, this trend did not mount to statistical significance and overall there was no significant difference in the growth of the primary tumors with any of the treatments (Figure 1A, B, and Supplementary Figure S2). Similarly, no significant inhibition of primary tumor growth was observed in the sunitinib sensitive or resistant RP-R-01 PDX models (Supplementary Figure S3A–C). In the RENCA model however, we observed a significant

reduction in final tumor weights in the trebananib treated group compared to vehicle but not in the combination group (Supplementary Figure 3D) which we speculate could be attributed to the distinct TME of a mouse tumor. Importantly, while the MET kinase inhibitor modestly restricted tumor growth in our spontaneously metastatic RP-R-02 LM model, the mice in this group had similar accumulation and diameter of lung metastases as the untreated cohort (Figure 1C). Strikingly, the overall number (Figure 1D) and diameter of lung metastases (Figure 1E) were significantly reduced after treatment with trebananib as compared to the vehicle. Further, the combination group had a significant reduction in the size of metastases as compared to vehicle and both single agent treatments, while reduction in metastases count was significantly reduced compared to vehicle and single agent MET Kinase inhibitor but not trebananib (Figure 1C–E). In summary, these data suggest that inhibition of the angiopoietin-TIE2-MET kinase axis may result in tumor microenvironment alterations which may hinder tumor metastasis.

Combination treatment hinders the metastatic potential of orthotopically implanted RP-R-02LM tumors.

To determine the effect of combination treatment on hindering tumor metastasis, we assessed the survival and metastatic burden of mice in vehicle, single agent, and combination groups. We implanted RP-R-02LM tumor pieces orthotopically, under the kidney capsule, and began treatment with AMG 386 at 5.6 mg/kg subcutaneously twice a week and/or 30 mg/kg MET kinase inhibitor at 4.5 weeks post-implantation – a time-point which we have shown metastases have begun to shed from the primary tumor to the lungs (35). We observed a significant increase in survival of mice in the combination group as compared to the vehicle cohort ($p < 0.0005$) while the single agent MET kinase cohort performed worse (median survival: vehicle – 183.5 days, trebananib – 161.5 days, MET kinase inhibitor 142 days, combination 218 days) (Figure 1F). These data suggest that, though in our initial studies (Figure 1A,B) we did not see a significant change in primary tumor growth, the significant decrease in metastatic burden that we observed in the trebananib and combination treatment (Figure 1D,E) could potentially be translated into a significant survival benefit as observed in the orthotopically implanted tumors.

Combination treatment hinders the metastatic potential of RP-R-02LM post tumor resection.

Clinically, RCC patients may have their primary tumor resected but they are still at risk to develop metastatic disease – most commonly to the lungs (39). To study the efficacy of trebananib in combination with MET kinase inhibition for the treatment of ccRCC, we implanted RP-R-02LM tumors subcutaneously and began treatment five and a half weeks post-implantation, a time point at which cells from the subcutaneous tumors begin to metastasize to the lungs (35). We then removed the primary tumor at 3 months post-implantation while continuing to treat the mice for the duration of the study. Our results showed a significant increase in survival of mice in the combination group compared to each cohort in the study with median survivals of 120 days vehicle, 168 days trebananib, 141 days MET kinase inhibitor, and 230 days – combination ($p < 0.0005$ combination – vehicle, $p < 0.005$ combination – MET kinase inhibitor and $p < 0.05$ combination – trebananib) (Figure 1G). In addition, we observed a significant delay in the development of lung metastases in

the combination cohort and strikingly less macro-metastases in the trebananib and combination cohorts as compared to the control and MET kinase inhibitor cohorts congruent with our initial studies (Supplementary Figure S4). These findings suggest that our combination therapy inhibits the ability of RP-R-02LM cells to settle in the lung niche. To better understand the molecular changes taking place in the primary tumors with the trebananib and MET kinase inhibitor combination we began to examine the molecular characteristics of EMT markers and the tumor microenvironment, with a focus on macrophage infiltration.

Markers of EMT are reduced by trebananib and c-MET inhibitor combined treatment.

Ang2-Tie2 signaling has been shown to promote metastasis through different mechanisms that include induction of tumor cell intravasation and dissemination (40,41), vascular destabilization (42) and induction of EMT (43). E-cadherin, which fails to be expressed in *VHL*-defective models of ccRCC, is a prognostic factor for patient survival (3,13). During the establishment and characterization of the RP-R-02LM model we observed changes in the expression of genes associated with metastases, including a significant increase in Snail expression and a decrease in E-cadherin (35) – changes that have been associated with tumor dissemination and subsequent establishment and growth in the metastatic niche. Based on these findings and consistent with our observation of extended survival in mice with orthotopic and subcutaneous RP-R-02LM tumors, we were interested in assessing the expression of E-cadherin to elucidate the impact of combination treatment on tumor dissemination. Tumor sample analysis yielded a trend towards increase in protein and RNA levels of E-cadherin and a statistically significant decrease in Snail RNA levels as well as vimentin protein levels in the combination treatment group relative to the vehicle cohort (Figure 2 A, B, and Supplementary Figure S5 A–C). The subcutaneous group, in which tumors were removed after only six and a half weeks of treatment, showed less of a trend of E-cadherin increase (Supplementary Figure S6) indicating that the impact of combination treatment on E-cadherin requires longer exposure of the primary tumor to treatment and alters the dissemination ability of the primary tumor. Next, we wanted to test the presence of tumor hypoxia which is known to be a key driver in renal cancer pathogenesis and a key mediator of aberrant angiogenesis (4,44). Using immunohistochemical staining for carbonic anhydrase-9 (CA-9), a well-established marker of hypoxia in renal cancer (45,46), we observed CA-9 expression to be significantly downregulated compared to vehicle control and single agent MET Kinase inhibitor (Figure 2C). Taken together, our data suggests that combination therapy promotes vascular normalization which improves tumor oxygenation and plays a role in hindering tumor dissemination and establishment of metastases in the lungs through the alteration of EMT markers.

Pathway activation downstream of Tie2 and c-MET is altered.

To elucidate whether we were hitting our target in the TME, we assessed the treatment effects on downstream effectors of the MET and Tie2 signaling pathways including AKT, STAT3 by Western blot analysis (Supplemental Figure S7A). We observed decreased AKT phosphorylation with single agent treatment as well as combination treatment (Supplemental Figure S7B–C). Decreased AKT phosphorylation upon treatment is indicative of successful target modulation, however associated changes in total AKT points towards more

complicated mechanism of action downstream of hitting both Tie2 and MET signaling pathways. We also examined p-STAT3, a marker of aggressiveness and proliferation (47), and noted that while there was an overall trend of p-STAT3 inhibition in the single agent and combination groups, there was no significant change from the vehicle (Supplemental Figure S7D). Previous studies have reported lack of correlation between Tie phosphorylation levels and targeting the angiotensin/Tie2 axis(48). Similarly, we did not detect a consistent trend in Tie phosphorylation changes in relation to neither type nor duration of treatment (Supplemental Figure S8). Taken together, these results suggest that we were capable of modulating signaling downstream of Tie2 and MET targeted inhibition both as single agents and when combined. However, modulation of AKT phosphorylation in treatment groups was not significantly different from vehicle control group when taking into account changes in total AKT. This was also true for changes in STAT phosphorylation. This may explain why, in the RP-R-02LM model, no significant difference was observed in the size of tumors in each treatment group at the end of treatment (Figure 1A, B). However, the benefit attained with the combination was limited to hindering tumor metastasis and prolonging survival which could be driven by alternative signaling mechanisms.

Combination treatment of the patient derived xenograft RP-R-02LM leads to enhanced pericyte coverage.

In addition to examining the EMT markers and downstream constituents of the MET and Tie2 pathways, we were interested in assessing the mechanism by which the combination treatment inhibits tumor metastases – as we were not seeing the expected inhibition of downstream markers in the combination treatment group. A possible explanation for inhibiting tumor metastasis is inducing vascular normalization. Vascular normalization is a multifactorial process that is assessed by examining vascular permeability, vascular sprouting and pericyte coverage (49,50). Therefore, we analyzed the presence of pericytes (NG2 staining) co-situated with endothelial cells (CD31 staining). Since the combination treatment of trebananib and MET kinase inhibitor may inhibit the dissemination of RP-R-02LM cells from the primary tumor to the lungs as well as decreases intra-tumor hypoxia despite continued growth of the primary tumor, we postulated that we might observe an alteration in the vasculature of the primary tumor. Indeed, we found that in the combination group there was a significant increase in the presence of NG2 positive pericytes co-localized with CD31 endothelial staining with an average Pearson Coefficient (R) of 0.842 in the combination compared to 0.60562 in the vehicle ($p < 0.05$) (Figure 3A–C). This increase of pericyte expression was verified by Western blot and densitometry analysis using ImageJ software (Figure 3D). These results indicate that the combination treatment of trebananib and MET kinase inhibitor may be strengthening the vasculature in a manner that functions as an anti-metastatic modulation of the tumor microenvironment. Taken together, these data indicate that inhibition of the angiotensin-TIE2-MET axis in our PDX model stabilizes blood vessels in the primary tumor and potently inhibits tumor cells metastases.

Tumor associated macrophage presence is significantly decreased with inhibition of the angiotensin-Tie2-cMET axis.

Tumor associated macrophages have been shown to facilitate tumor metastases *via* promotion of tissue remodeling, angiogenesis, and production of extra cellular matrix

remodeling enzymes, such as matrix metalloproteinases (5,6). We hypothesized that perivascular, tumor associated macrophages, angiopoietin receptor Tie2⁺ cells, which are known to mediate tumor metastases(4), may be reduced in the tumor microenvironment of our combination group. To test this hypothesis, we examined tumors from our *in vivo* subcutaneous study of RP-R-02LM, for Tie2, F4/80 pan-macrophage marker, and CD206 M2-like macrophage marker. In the combination cohort, there was a significant decrease in the presence of TAMs (F480⁺Tie2⁺CD206⁺) in the tumor microenvironment in comparison to vehicle control (Figure 4A, B, Supplemental Figure S9, 10). We found that in both control, single agent and combination treated groups there was a significant co-localization of Tie2/CD206 (Pearson's coefficient = 0.9) (Figure 4C), confirming the presence of Tie2⁺ macrophages in our tumors. These data show that combination treatment of trebananib and MET kinase inhibitor inhibits the infiltration of M2-like TAMs into the tumor microenvironment, suggesting a potential role for these TAMs in the metastases of the PDX model RP-R-02LM.

DISCUSSION

Successful treatment of cancer patients with metastatic disease remains one of the most daunting tasks for clinicians managing solid tumors, including ccRCC (17,30). Despite the recent surge of research contributing to the understanding of metastatic disease and its interaction with stroma, there is much work to be done to translate these advances into the clinic (17,30). In our study, we assessed the effect of the Ang1/Ang2 peptibody, trebananib, as a single agent and in combination with inhibition of the MET kinase pathway. Our data show evidence that this combination may alter both the tumor niche and microenvironment through the alteration of pericytes and inhibition of metastases promoting macrophages in a metastatic ccRCC PDX model (4–8,51).

The MET kinase pathway is often over-activated in *VHL* negative ccRCC tumors, as reflected also in our RP-R-02LM model compared to the parental non-metastatic RP-R-02 PDX (51). MET kinase over-activation leads to worse patient survival and a more aggressive and invasive phenotype (3,32,52,53). Additionally, inhibition of MET has been shown to be sufficient to subdue HGF dependent migration and downstream targets, such as ERK and AKT (32). Thus, MET kinase inhibition is a promising target for metastatic ccRCC and cabozantinib, a multi-kinase inhibitor with activity against MET, has recently been approved for RCC patients (54). Trebananib, a recombinant peptide-Fc fusion protein which negates the receptor/ligand interaction of Ang1/Ang2 with the Tie2 receptor, has been reported to improve progression-free survival (PFS) in patients with ovarian cancer in a phase III trial as compared with paclitaxel (55). In our studies, we assessed the combination of MET kinase inhibition with trebananib in both murine and patient derived xenograft models of RCC. Although our combination treatment studies did not yield a significant difference in primary tumor growth compared to the single agent treatments, we observed a significant inhibition of metastases, a trend of increased expression of the epithelial marker E-cadherin albeit non statistically significant, a reduction of mesenchymal marker Snail, upregulated pericyte coverage, improved intra-tumor oxygenation and reduced presence of metastases promoting M2-like macrophages in the primary tumor of our metastatic ccRCC PDX model, RP-R-02LM. These results suggest that in our models combination of MET kinase inhibition

and angiopoietin inhibition may not provide an advantage in inhibition of primary tumor growth as compared with single agent treatments alone. In contrast, trebananib treatment combined with MET kinase inhibition in our metastatic PDX model, RP-R-02LM, not only decreased the presence of tumor metastases to the lungs but also significantly enhanced survival. In this highly metastatic model we observed the need to inhibit both the angiopoietin/Tie2 axis and the MET axis concomitantly to significantly affect the metastatic burden and survival.

In our initial short term treatment study with the highly metastatic RP-R-02LM model, we noted a significant decrease in metastases to the lungs, indicating that we were impairing the metastatic potential of the tumor. In our orthotopic study, we noted that when RP-R-02LM tumor pieces were implanted into the kidney and treated for at least 4 months a significant improvement in survival in the combination groups were observed. The mice in the combination group died of their primary tumor growth and not their metastatic burden while those in the vehicle and c-MET inhibition group died of metastatic burden. In our subcutaneous study, we removed the primary tumors at 3 months post-implantation, a time which we have shown that these tumors have already shed metastatic cells (35), continued to treat the mice, and assessed for metastatic burden. We found that the combination group had a striking increase in survival compared to both single agent and vehicle cohorts. These findings together suggest that combining Ang1/Ang2 inhibition with c-MET inhibition results in significant decrease in metastasis and thus prolonged survival.

Blood vessel normalization and increased pericyte coverage have traditionally been viewed as tumor promoting. However, recent literature has suggested a dual role (22,56). Studies have shown that increased blood vessel stabilization, E-cadherin restoration, reduced presence of perivascular macrophages, and pericyte coverage in multiple cancer types contribute to reduced metastases and prolonged survival (4,5,8,15,56). These studies elucidate the vital role of macrophage and pericyte recruitment on blood vessel normalization in the tumor microenvironment (4,5,7,8,15). Additionally, clinical evidence shows in colorectal and RCC patients that reduced macrophage and increased micro vessel pericyte coverage correlates with increased overall patient survival and a reduction in metastases (5,15,57,58). Our results indicate that pericyte coverage, reduced macrophage presence, and stabilization of tumor vasculature in combination cohort may contribute to prolonged survival and reduced lung metastases in ccRCC. These results further emphasize the potential of MET kinase and angiopoietin inhibition to affect the tumor microenvironment in a manner that significantly inhibits the metastatic phenotype of ccRCC.

Therapeutic treatments for ccRCC patients are rapidly evolving. Recently, two RTKIs (receptor tyrosine kinase inhibitors), cabozantinib and lenvatinib have been approved for use in the treatment of metastatic, RTKIs resistant disease. However, to date the use of RTKIs in the adjuvant setting remains controversial as studies have shown discordant results (59) (60). Our preclinical studies suggest a selective anti-metastatic effect of concomitant angiopoietin1/2 and c-MET inhibition. This observation provides the rationale for developing selective inhibitors for these pathways to be tested in the adjuvant setting. This is

clinically relevant since small molecules that inhibit both Tie2 and MET are currently in clinical testing.

In conclusion, targeting the tumor microenvironment and the tumor niche *via* combination of a small molecule MET kinase inhibitor with the peptide inhibitor of angiotensin 1/2, trebananib has striking biological effects. In our metastatic patient-derived xenograft ccRCC model, RP-R-02LM, this combination suppressed both tumor metastases, and enhanced survival. In addition, the combination resulted in blood vessel stabilization, reduced tumor promoting macrophage presence, increased pericyte coverage and showed a trend of increased E-cadherin expression albeit not statistically significant. The combination treatment inhibited upregulation of mesenchymal markers, reduced M2-like macrophage presence and increased the pericyte coverage within the tumor, suggesting a less permissive environment for the escape of metastatic cells from the primary tumor microenvironment. Taken together, these results suggest that combining angiotensin/TIE2 inhibition with MET kinase inhibition may be a clinically effective adjuvant therapy for patients with ccRCC.

Supplementary Material

Refer to Web version on PubMed Central for supplementary material.

ACKNOWLEDGMENTS

This study was in part supported by a research grant from Amgen, the National Institutes of Health-National Cancer Institute (P30CA082709), and a donation from the late Dr. Richard Turner and Mrs. Deidre Turner.

Conflict of interest: This study was supported in part by a research grant from Amgen (R.P.). A. Coxon, K. Rex and S. Caenepeel are all employees and shareholders of Amgen Inc.

REFERENCES

- Jonasch E, Gao J, Rathmell WK. Renal cell carcinoma. *BMJ* 2014;349:g4797 doi 10.1136/bmj.g4797. [PubMed: 25385470]
- Society AC. Kidney Cancer (Adult) - Renal Cell Carcinoma. American Cancer Society 2016.
- Esteban MA, Tran MG, Harten SK, Hill P, Castellanos MC, Chandra A, et al. Regulation of E-cadherin expression by VHL and hypoxia-inducible factor. *Cancer Res* 2006;66(7):3567–75 doi 10.1158/0008-5472.CAN-05-2670. [PubMed: 16585181]
- Kadioglu E, De Palma M. Cancer Metastasis: Perivascular Macrophages Under Watch. *Cancer Discov* 2015;5(9):906–8 doi 10.1158/2159-8290.CD-15-0819. [PubMed: 26334045]
- Kovaleva OV, Samoilova DV, Shitova MS, Gratchev A. Tumor Associated Macrophages in Kidney Cancer. *Anal Cell Pathol (Amst)* 2016;2016:9307549 doi 10.1155/2016/9307549. [PubMed: 27807511]
- Pollard JW. Tumour-educated macrophages promote tumour progression and metastasis. *Nat Rev Cancer* 2004;4(1):71–8. [PubMed: 14708027]
- Thurston G, Daly C. The complex role of angiotensin-2 in the angiotensin-tie signaling pathway. *Cold Spring Harb Perspect Med* 2012;2(9):a006550 doi 10.1101/cshperspect.a006550. [PubMed: 22951441]
- Xian X, Hakansson J, Stahlberg A, Lindblom P, Betsholtz C, Gerhardt H, et al. Pericytes limit tumor cell metastasis. *J Clin Invest* 2006;116(3):642–51 doi 10.1172/JCI25705. [PubMed: 16470244]
- Arwert EN, Harney AS, Entenberg D, Wang Y, Sahai E, Pollard JW, et al. A Unidirectional Transition from Migratory to Perivascular Macrophage Is Required for Tumor Cell Intravasation. *Cell reports* 2018;23(5):1239–48. [PubMed: 29719241]

10. Benest AV, Kruse K, Savant S, Thomas M, Laib AM, Loos EK, et al. Angiopoietin-2 is critical for cytokine-induced vascular leakage. *PLoS One* 2013;8(8):e70459 doi 10.1371/journal.pone.0070459. [PubMed: 23940579]
11. Roodhart JM, He H, Daenen LG, Monvoisin A, Barber C, Van Amersfoort M, et al. Notch1 regulates angio-supportive bone marrow-derived cells: relevance to chemoresistance. *Blood* 2013;blood-2012-11-459347.
12. Mazzieri R, Pucci F, Moi D, Zonari E, Raghetti A, Berti A, et al. Targeting the ANG2/TIE2 axis inhibits tumor growth and metastasis by impairing angiogenesis and disabling rebounds of proangiogenic myeloid cells. *Cancer cell* 2011;19(4):512–26. [PubMed: 21481792]
13. Cai J Roles of transcriptional factor Snail and adhesion factor E-cadherin in clear cell renal cell carcinoma. *Exp Ther Med* 2013;6(6):1489–93 doi 10.3892/etm.2013.1345. [PubMed: 24255679]
14. Keskin D, Kim J, Cooke VG, Wu CC, Sugimoto H, Gu C, et al. Targeting vascular pericytes in hypoxic tumors increases lung metastasis via angiopoietin-2. *Cell Rep* 2015;10(7):1066–81 doi 10.1016/j.celrep.2015.01.035. [PubMed: 25704811]
15. Meng MB, Zaorsky NG, Deng L, Wang HH, Chao J, Zhao LJ, et al. Pericytes: a double-edged sword in cancer therapy. *Future Oncol* 2015;11(1):169–79 doi 10.2217/fon.14.123. [PubMed: 25143028]
16. Minami Y, Sasaki T, Kawabe J-i, Ohsaki Y. Accessory Cells in Tumor Angiogenesis — Tumor-Associated Pericytes. 2013 doi 10.5772/54523.
17. Wan L, Pantel K, Kang Y. Tumor metastasis: moving new biological insights into the clinic. *Nat Med* 2013;19(11):1450–64 doi 10.1038/nm.3391. [PubMed: 24202397]
18. Coffelt SB, Tal AO, Scholz A, De Palma M, Patel S, Urbich C, et al. Angiopoietin-2 regulates gene expression in TIE2-expressing monocytes and augments their inherent proangiogenic functions. *Cancer Res* 2010;70(13):5270–80 doi 10.1158/0008-5472.CAN-10-0012. [PubMed: 20530679]
19. Kobayashi H, DeBusk LM, Babichev YO, Dumont DJ, Lin PC. Hepatocyte growth factor mediates angiopoietin-induced smooth muscle cell recruitment. *Blood* 2006;108(4):1260–6 doi 10.1182/blood-2005-09-012807. [PubMed: 16638932]
20. Marchetti C, Gasparri ML, Ruscito I, Palaia I, Perniola G, Carrone A, et al. Advances in anti-angiogenic agents for ovarian cancer treatment: The role of trebananib (AMG 386). *Crit Rev Oncol Hematol* 2015;94(3):302–10 doi 10.1016/j.critrevonc.2015.02.001. [PubMed: 25783620]
21. Huang H, Bhat A, Woodnutt G, Lappe R. Targeting the ANGPT-TIE2 pathway in malignancy. *Nat Rev Cancer* 2010;10(8):575–85 doi 10.1038/nrc2894. [PubMed: 20651738]
22. Falcón BL, Hashizume H, Koumoutsakos P, Chou J, Bready JV, Coxon A, et al. Contrasting actions of selective inhibitors of angiopoietin-1 and angiopoietin-2 on the normalization of tumor blood vessels. *The American journal of pathology* 2009;175(5):2159–70. [PubMed: 19815705]
23. Shim WS, Teh M, Bapna A, Kim I, Koh G-Y, Mack PO, et al. Angiopoietin 1 promotes tumor angiogenesis and tumor vessel plasticity of human cervical cancer in mice. *Experimental cell research* 2002;279(2):299–309. [PubMed: 12243755]
24. Shim WS, Teh M, Mack PO, Ge R. Inhibition of angiopoietin-1 expression in tumor cells by an antisense RNA approach inhibited xenograft tumor growth in immunodeficient mice. *International journal of cancer* 2001;94(1):6–15. [PubMed: 11668472]
25. Coxon A, Bready J, Min H, Kaufman S, Leal J, Yu D, et al. Context-Dependent Role of Angiopoietin-1 Inhibition in the Suppression of Angiogenesis and Tumor Growth: Implications for AMG 386, an Angiopoietin-1/2–Neutralizing Peptibody. *Molecular cancer therapeutics* 2010;9(10):2641–51. [PubMed: 20937592]
26. Sierra J, Tsao M. c-MET as a potential therapeutic target and biomarker in cancer. *Therapeutic Advances in Medical Oncology* 2011;3(S1):S21–S35 doi 10.1177/1758834011422557. [PubMed: 22128285]
27. Ciamporcerio E, Miles KM, Adelaiye R, Ramakrishnan S, Shen L, Ku S, et al. Combination strategy targeting VEGF and HGF/c-met in human renal cell carcinoma models. *Mol Cancer Ther* 2015;14(1):101–10 doi 10.1158/1535-7163.MCT-14-0094. [PubMed: 25381264]
28. Finisguerra V, Prenen H, Mazzone M. Preclinical and clinical evaluation of MET functions in cancer cells and in the tumor stroma. *Oncogene* 2016 doi 10.1038/onc.2016.36.

29. Spina A, De Pasquale V, Cerulo G, Cocchiario P, Della Morte R, Avallone L, et al. HGF/c-MET Axis in Tumor Microenvironment and Metastasis Formation. *Biomedicines* 2015;3(1):71–88 doi 10.3390/biomedicines3010071. [PubMed: 28536400]
30. Chen SC, Kuo PL. Bone Metastasis from Renal Cell Carcinoma. *Int J Mol Sci* 2016;17(6) doi 10.3390/ijms17060987.
31. Piao Y, Park SY, Henry V, Smith BD, Tiao N, Flynn DL, et al. Novel MET/TIE2/VEGFR2 inhibitor altiratinib inhibits tumor growth and invasiveness in bevacizumab-resistant glioblastoma mouse models. *Neuro Oncol* 2016 doi 10.1093/neuonc/now030.
32. Xie Z, Lee YH, Boeke M, Jilaveanu LB, Liu Z, Bottaro DP, et al. MET Inhibition in Clear Cell Renal Cell Carcinoma. *J Cancer* 2016;7(10):1205–14 doi 10.7150/jca.14604. [PubMed: 27390595]
33. Boezio AA, Berry L, Albrecht BK, Bauer D, Bellon SF, Bode C, et al. Discovery and optimization of potent and selective triazolopyridazine series of c-Met inhibitors. *Bioorg Med Chem Lett* 2009;19(22):6307–12 doi 10.1016/j.bmcl.2009.09.096. [PubMed: 19819693]
34. Adelaiye R, Ciamporcerio E, Miles KM, Sotomayor P, Bard J, Tsompana M, et al. Sunitinib dose escalation overcomes transient resistance in clear cell renal cell carcinoma and is associated with epigenetic modifications. *Mol Cancer Ther* 2015;14(2):513–22 doi 10.1158/1535-7163.MCT-14-0208. [PubMed: 25519701]
35. Adelaiye-Ogala R, Budka J, Damayanti NP, Arrington J, Ferris M, Hsu CC, et al. EZH2 Modifies Sunitinib Resistance in Renal Cell Carcinoma by Kinome Reprogramming. *Cancer Res* 2017;77(23):6651–66 doi 10.1158/0008-5472.CAN-17-0899. [PubMed: 28978636]
36. Ruifrok AC, Johnston DA. Quantification of histochemical staining by color deconvolution. *Analytical and quantitative cytology and histology* 2001;23(4):291–9. [PubMed: 11531144]
37. Kato Y, Yoshimura K, Shin T, Verheul H, Hammers H, Sanni TB, et al. Synergistic in vivo antitumor effect of the histone deacetylase inhibitor MS-275 in combination with interleukin 2 in a murine model of renal cell carcinoma. *Clin Cancer Res* 2007;13(15 Pt 1):4538–46 doi 10.1158/1078-0432.CCR-07-0014. [PubMed: 17671140]
38. Molina AM, Jia X, Feldman DR, Hsieh JJ, Ginsberg MS, Velasco S, et al. Long-term response to sunitinib therapy for metastatic renal cell carcinoma. *Clin Genitourin Cancer* 2013;11(3):297–302 doi 10.1016/j.clgc.2013.04.001. [PubMed: 23707221]
39. Chin AI, Lam JS, Figlin RA, Belldgrun AS. Surveillance strategies for renal cell carcinoma patients following nephrectomy. *Rev Urol* 2006;8(1):1–7. [PubMed: 16985554]
40. Harney AS, Arwert EN, Entenberg D, Wang Y, Guo P, Qian B-Z, et al. Real-time imaging reveals local, transient vascular permeability, and tumor cell intravasation stimulated by TIE2hi macrophage-derived VEGFA. *Cancer discovery* 2015.
41. Karagiannis GS, Pastoriza JM, Wang Y, Harney AS, Entenberg D, Pignatelli J, et al. Neoadjuvant chemotherapy induces breast cancer metastasis through a TMEM-mediated mechanism. *Science translational medicine* 2017;9(397):ean0026. [PubMed: 28679654]
42. Peterson TE, Kirkpatrick ND, Huang Y, Farrar CT, Marijt KA, Kloepper J, et al. Dual inhibition of Ang-2 and VEGF receptors normalizes tumor vasculature and prolongs survival in glioblastoma by altering macrophages. *Proceedings of the National Academy of Sciences* 2016;113(16):4470–5.
43. Imanishi Y, Hu B, Jarzynka MJ, Guo P, Elishaev E, Bar-Joseph I, et al. Angiopoietin-2 stimulates breast cancer metastasis through the $\alpha 5\beta 1$ integrin-mediated pathway. *Cancer Research* 2007;67(9):4254–63. [PubMed: 17483337]
44. Schödel J, Grampp S, Maher ER, Moch H, Ratcliffe PJ, Russo P, et al. Hypoxia, hypoxia-inducible transcription factors, and renal cancer. *European urology* 2016;69(4):646–57. [PubMed: 26298207]
45. Tostain J, Li G, Gentil-Perret A, Gigante M. Carbonic anhydrase 9 in clear cell renal cell carcinoma: a marker for diagnosis, prognosis and treatment. *European journal of cancer* 2010;46(18):3141–8. [PubMed: 20709527]
46. Genega EM, Ghebremichael M, Najarian R, Fu Y, Wang Y, Argani P, et al. Carbonic anhydrase IX expression in renal neoplasms: correlation with tumor type and grade. *American journal of clinical pathology* 2010;134(6):873–9. [PubMed: 21088149]
47. Dunkel Y, Ong A, Notani D, Mittal Y, Lam M, Mi X, et al. STAT3 protein up-regulates Galpha-interacting vesicle-associated protein (GIV)/Girdin expression, and GIV enhances STAT3

- activation in a positive feedback loop during wound healing and tumor invasion/metastasis. *J Biol Chem* 2012;287(50):41667–83 doi 10.1074/jbc.M112.390781. [PubMed: 23066027]
48. Grenga I, Kwilas AR, Donahue RN, Farsaci B, Hodge JW. Inhibition of the angiopoietin/Tie2 axis induces immunogenic modulation, which sensitizes human tumor cells to immune attack. *J Immunother Cancer* 2015;3:52 doi 10.1186/s40425-015-0096-7. [PubMed: 26579226]
 49. Maione F, Giraudo E. Tumor angiogenesis: methods to analyze tumor vasculature and vessel normalization in mouse models of cancer. *Mouse Models of Cancer*: Springer; 2015 p 349–65.
 50. Chauhan VP, Stylianopoulos T, Martin JD, Popovi Z, Chen O, Kamoun WS, et al. Normalization of tumour blood vessels improves the delivery of nanomedicines in a size-dependent manner. *Nature nanotechnology* 2012;7(6):383–8.
 51. Adelaiye R, Chintala S, Orillion A, Pettazzoni P, Elbanna M, Arisa S, et al. Androgen receptor expression is associated with sunitinib resistance in renal cell carcinoma models. *Proc AACR* #21262016.
 52. Baldewijns M, van Vlodrop I, Vermeulen P, Soetekouw P, van Engeland M, de Brüne A. VHL and HIF signalling in renal cell carcinogenesis. *Journal of Pathology* 2010;221:125–38 doi 10.1002/path.2689. [PubMed: 20225241]
 53. Oh R, Park J, Lee J, Shin M, Kim H, Lee S, et al. Expression of HGF/SF and Met protein is associated with genetic alterations of VHL gene in primary renal cell carcinomas. *Acta Pathol Microbiol Immunol Scand* 2002;110:229–38.
 54. Choueiri TK, Escudier B, Powles T, Tannir NM, Mainwaring PN, Rini BI, et al. Cabozantinib versus everolimus in advanced renal cell carcinoma (METEOR): final results from a randomised, open-label, phase 3 trial. *Lancet Oncol* 2016;17(7):917–27 doi 10.1016/S1470-2045(16)30107-3. [PubMed: 27279544]
 55. Fujiwara K, Monk BJ, Lhomme C, Coleman RL, Brize A, Oaknin A, et al. Health-related quality of life in women with recurrent ovarian cancer receiving paclitaxel plus trebananib or placebo (TRINOVA-1). *Ann Oncol* 2016;27(6):1006–13 doi 10.1093/annonc/mdw147. [PubMed: 27029706]
 56. Agrawal V, Maharjan S, Kim K, Kim N, Son J, Lee K, et al. Direct endothelial junction restoration results in significant tumor vascular normalization and metastasis inhibition in mice. *Oncotarget* 2014;5(9):2761–77. [PubMed: 24811731]
 57. Qian CN, Huang D, Wondergem B, Teh BT. Complexity of tumor vasculature in clear cell renal cell carcinoma. *Cancer* 2009;115(10 Suppl):2282–9 doi 10.1002/cncr.24238. [PubMed: 19402071]
 58. Yonenaga Y, Mori A, Onodera H, Yasuda S, Oe H, Fujimoto A, et al. Absence of smooth muscle actin-positive pericyte coverage of tumor vessels correlates with hematogenous metastasis and prognosis of colorectal cancer patients. *Oncology* 2005;69(2):159–66 doi 10.1159/000087840. [PubMed: 16127287]
 59. Haas NB, Manola J, Uzzo RG, Flaherty KT, Wood CG, Kane C, et al. Adjuvant sunitinib or sorafenib for high-risk, non-metastatic renal-cell carcinoma (ECOG-ACRIN E2805): a double-blind, placebo-controlled, randomised, phase 3 trial. *Lancet* 2016;387(10032):2008–16 doi 10.1016/S0140-6736(16)00559-6. [PubMed: 26969090]
 60. Motzer RJ, Ravaud A, Patard JJ, Pandha HS, George DJ, Patel A, et al. Adjuvant Sunitinib for High-risk Renal Cell Carcinoma After Nephrectomy: Subgroup Analyses and Updated Overall Survival Results. *Eur Urol* 2018;73(1):62–8 doi 10.1016/j.eururo.2017.09.008. [PubMed: 28967554]

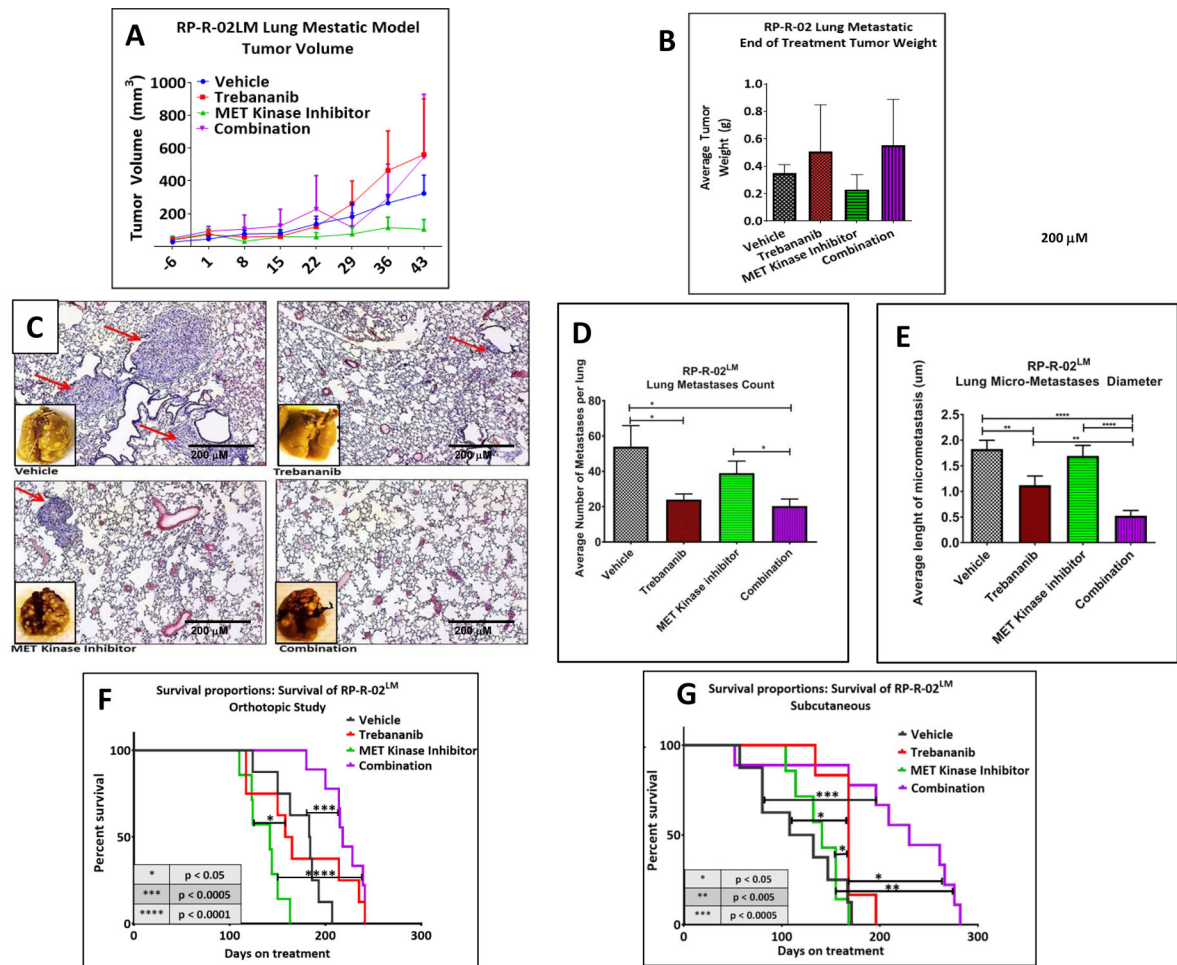


Figure 1. Combination treatment of trebananib and MET kinase inhibitor results in significant inhibition of metastases and increased survival in the metastatic RP-R-02LM.

(A) Non survival subcutaneous study tumor growth curves show no significant difference across the cohorts. (B) Non survival subcutaneous study end-point tumor weights show no significant difference in tumor size ($n = 6$ mice per group). (C) Non survival subcutaneous study representative H&E staining of the lungs show a striking reduction in the presence of lung metastases in the trebananib and combination groups. Scale bar = $200 \mu\text{m}$ (D-E) Non survival subcutaneous study, blinded analysis of the average number of lung metastases and metastatic diameter showed a significant reduction in the presence of metastases in the combination group as compared to all other groups ($n = 6$ mice per group; $n = 136$ – 173 images per group). (F) Orthotopic study-Kaplan-Meier survival curve showing a significant increase in the survival of both the combination and trebananib treatment alone compared to the vehicle cohort. (G) Subcutaneous study-Kaplan-Meier survival curve revealing a strikingly significant increase in the survival rates of mice in the combination group as compared to all other groups in the study. Results are given as mean + SEM. * p -value = <0.05 , ** p -value = <0.005 , *** p -value = <0.001 , **** p -value = <0.0001 .

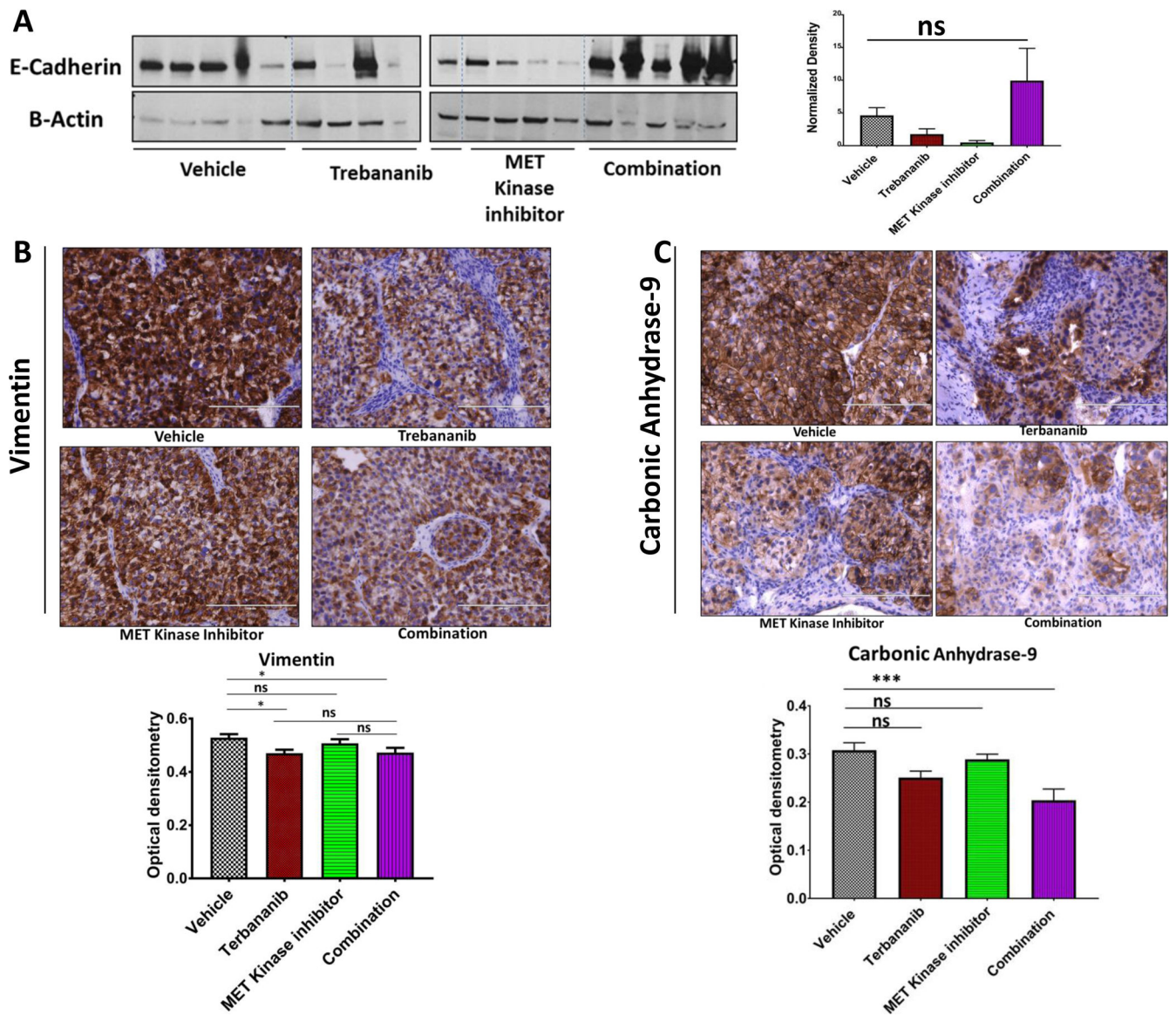


Figure 2. Increased survival with trebananib and a MET kinase inhibitor is associated with increased presence of the epithelial marker E-cadherin.

(A) Western blot analysis of epithelial marker E-cadherin in tumor lysates derived from mice in the orthotopic study in each treatment group ($n = 4-5$ mice per group). Western blot densitometry analysis shows trend towards increase in the presence of E-cadherin in the combination group compared to other groups ($n = 5$ mice per group). (B) Representative images of tumors from each treatment group in the orthotopic study stained for vimentin expression with IHC. Optical densitometry analysis of all images (5 mice per group; 25–30 images per group) shows a significant decrease of vimentin expression in combination and single agent trebananib groups compared to vehicle control. Scale bar= 200 μm (C) Representative images of tumors from each treatment group in the orthotopic study stained for CA-9 expression with IHC. Optical densitometry analysis of all images (5 mice per group; 25–30 images per group) shows a significant decrease of CA-9 expression in

combination group compared to vehicle control. Results are given as mean + SEM. *p-value = <0.05, **p-value = <0.005, ***p-value = <0.001, ****p-value = <0.0001.

Author Manuscript

Author Manuscript

Author Manuscript

Author Manuscript

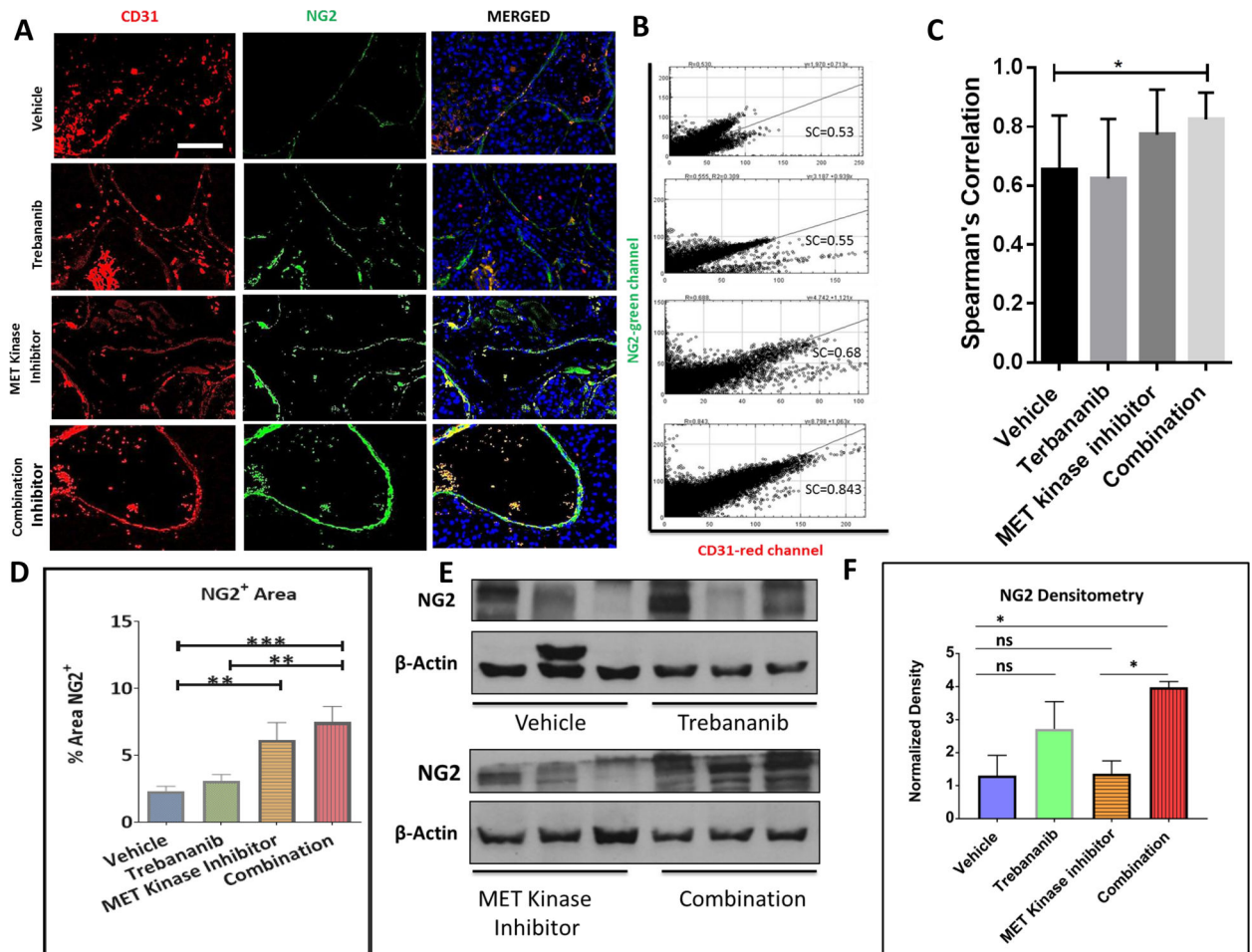


Figure 3. Treatment of RP-R-02LM tumors (Orthotopic study) with trebananib and MET kinase inhibitor results in increased pericyte coverage of the tumor vasculature.

(A) Immunofluorescent staining pattern for CD31 (red), NG2 (green), and DAPI (blue) in different treatment groups. (B, C) Confocal images of vehicle and combination treatment groups suggest more functional and stable vasculature in the combination group (left). Scale bar = 200 μ m. Blinded co-localization analysis (Spearman's correlation) reveals a statistically significant, $p < 0.05$, increase in NG2⁺ CD31⁺ co-localized cells in the combination cohort (right) ($n = 23$ – 33 images per group). (D) Blinded assessment of the positive areas for NG2 co-verifies the IF staining in Figure 4A, revealing a significant increase in pericyte coverage in the combination group ($n = 20$ – 25 images per group). (E, F) Western blot analysis and densitometry data show a significant increase in the presence of pericyte marker NG2 in the combination group as compared to the vehicle and MET kinase inhibitor treatment groups ($n = 4$ – 5 mice per group).

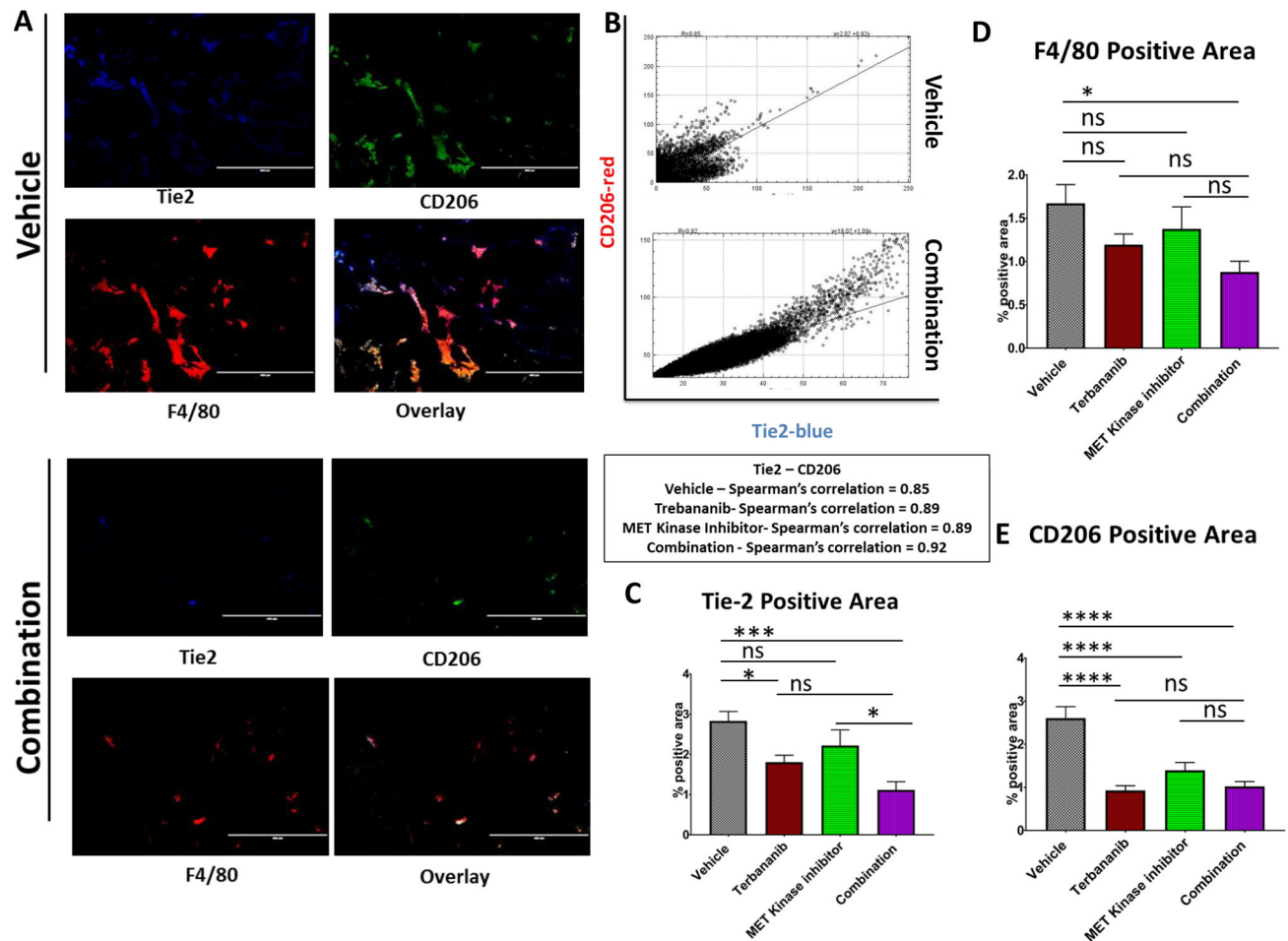


Figure 4. Concomitant inhibition of the angiopoietin-TIE2 axis and the MET kinase pathway in RP-R-02LM tumors (Orthotopic study) yields significant alterations in pro-tumor macrophages. (A) Single stain and merge of TIE2⁺ (blue) M2-like, tumor promoting macrophages (CD206⁺F4/80⁺ - green/red) reveals a significant reduction in the presence of M2-like tumor associated macrophages in the combination treatment cohort. Scale bar= 400 μ m (B) TIE2+CD206+ co-localization indicates the potential for combination treatment to directly impact the presence of TAMs in the tumor microenvironment. Spearman's correlation coefficient for all treatment groups \approx 0.9. Spearman's correlation coefficient was calculated by using imageJ coloc2 across different treatment conditions. (C, D, E) Blinded quantitation of the immunofluorescent staining reveals a statistically significant reduction in TAMs (TIE2⁺F4/80⁺CD206⁺) in the tumor microenvironment. (n = 30–40 images per group).